OPEN

Rapid fabrication of self-ordered porous alumina with 10-/sub-10-nm-scale nanostructures by selenic acid anodizing

Osamu Nishinaga, Tatsuya Kikuchi, Shungo Natsui & Ryosuke O. Suzuki

Faculty of Engineering, Hokkaido University, N13-W8, Kita-ku, Sapporo, Hokkaido, 060-8628, Japan.

Anodic porous alumina has been widely investigated and used as a nanostructure template in various nanoapplications. The porous structure consists of numerous hexagonal cells perpendicular to the aluminum substrate and each cell has several tens or hundreds of nanoscale pores at its center. Because the nanomorphology of anodic porous alumina is limited by the electrolyte during anodizing, the discovery of additional electrolytes would expand the applicability of porous alumina. In this study, we report a new self-ordered nanoporous alumina formed by selenic acid (H_2SeO_4) anodizing. By optimizing the anodizing conditions, anodic alumina possessing 10-nm-scale pores was rapidly assembled (within 1 h) during selenic acid anodizing without any special electrochemical equipment. Novel sub-10-nm-scale spacing can also be achieved by selenic acid anodizing and metal sputter deposition. Our new nanoporous alumina can be used as a nanotemplate for various nanostructures in 10-/sub-10-nm-scale manufacturing.

In recent years, the structural control of anodic porous alumina has been widely investigated for use in items such as templates, filters, magnetic recording media, photonic crystals, and plasmonic devices[1–11]. The porous structure consists of numerous hexagonal cells perpendicular to the aluminum substrate and each cell has several tens or hundreds of nanoscale pores at its center[12–14]. Porous alumina can be obtained from aluminum via anodizing in one of several available acidic electrolytes, and the nanostructural features of the porous alumina are determined by the chosen electrolyte and the applied anodizing potential[4,15,16]. Specifically, self-ordered porous alumina is typically obtained via anodizing in the following three types of electrolyte under an appropriate applied voltage for several hours or days: a) sulfuric acid (H_2SO_4) at 19–27 V; b) oxalic acid (($COOH)_2$) at 40 V; and c) phosphoric acid (H_3PO_4) at 160–195 V[4]. Using this technique, the interpore distance (D_{int}, identical meaning to cell size) of the porous alumina is proportional to the applied voltage with a proportional constant $k = 2.5$ nm V^{-1}. These anodizing electrolytes were patented and reported in the 1920s to 1940s for the surface finishing of aluminum and its alloys to improve their chemical and mechanical properties[17], and they remain well-known, self-ordering electrolytes for porous alumina fabrication[18]. Malonic acid ($HOOC$-CH_2-$COOH$) and tartaric acid ($HOOC(CHOH)_2COOH$), dicarboxylic acids, were reported for porous alumina by the 1970s, and also afford self-ordering porous alumina at 120 V and 195 V, respectively[19]. In addition to these five electrolytes, several other anodizing solutions, including chromic, malic, citric, and glycolic acids, have been reported for anodic porous alumina fabrication[16,20–22]. However, obtaining a self-ordered porous alumina is difficult because of branching colony-forming nanostructures or the high electric fields required for anodizing (more than 200 V). Therefore, the potential applications of anodic porous alumina are limited by the narrow range of five self-ordering electrolytes (especially, sulfuric, oxalic, and phosphoric acids).

In this study, we report a self-ordered porous alumina formed via anodizing in a new self-ordered electrolyte, selenic acid (H_2SeO_4). This interesting inorganic electrolyte rapidly establishes self-ordering hexagonal cells within 1 h, which is more than 10-fold faster than the self-ordering times required in sulfuric, oxalic, and phosphoric acids[23–25]. In addition, selenic acid anodizing works effectively at a previously unutilized self-ordering voltage (48 V) with 110 nm cell size. This self-ordered porous alumina can be obtained using a simple electro-chemical setup (Supplementary Fig. S1) without the powerful cooling stage employed in hard anodizing or other previously reported setups[4]. Finally, the obtained self-ordered porous alumina had a 10-nm-scale pore diameter, the smallest reported value thus far[26,27]. This novel anodic alumina allowed the fabrication of single nanometer-sized nanostructures.
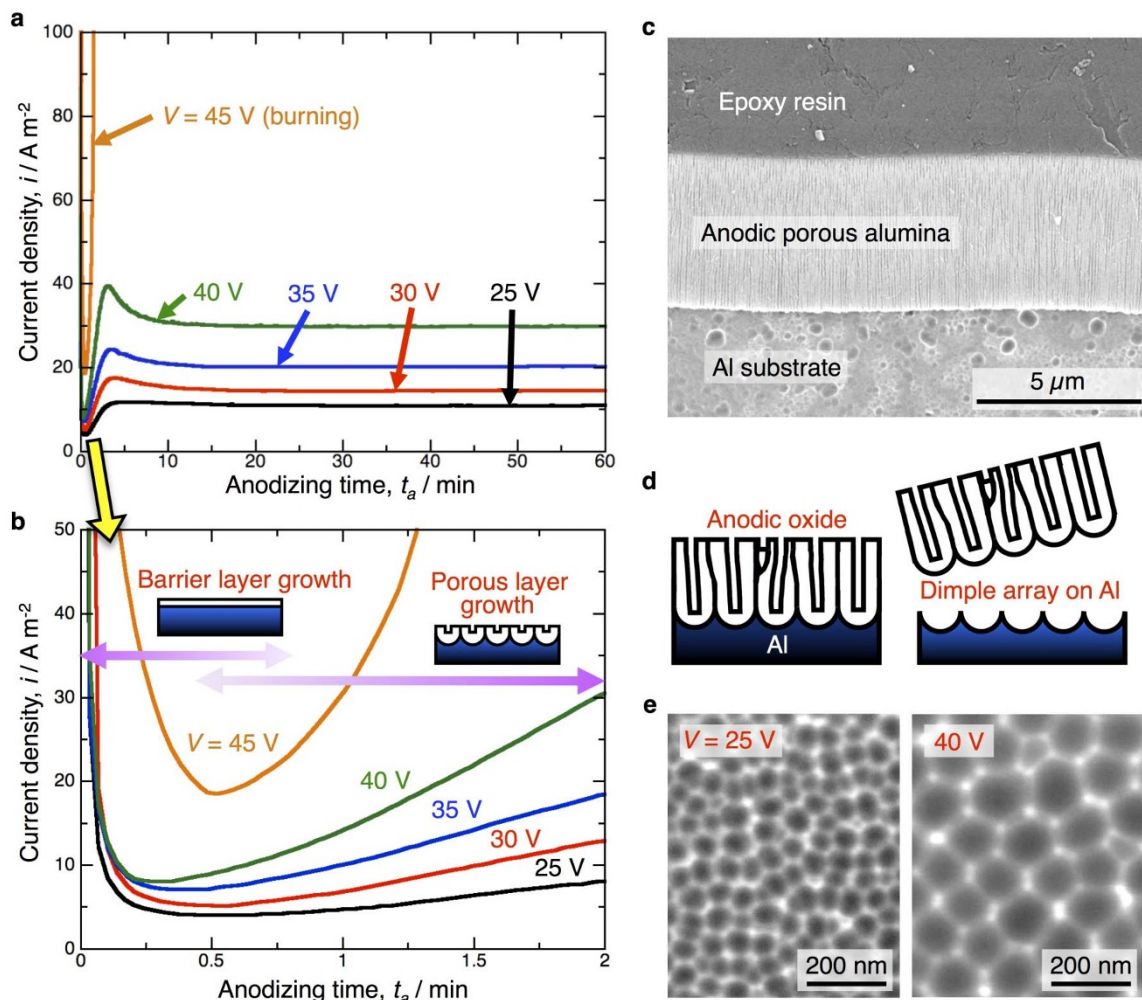
Figure 1 | Anodizing in a selenic acid solution at 293 K. (a), Current density changes with anodizing time in a 0.3 M selenic acid solution (293 K) at different constant voltages of 25–45 V. (b), Current-time transients in the initial stage of a). Schematic models of barrier and porous oxide film formation on aluminum are also shown in the figure. (c), SEM images of the vertical cross-section of a specimen via typical anodizing. The specimen was embedded onto an epoxy resin and then polished mechanically. (d), Schematic models of anodic porous alumina formed on the aluminum substrate and nanodimple array formed on the oxide/metal interface. (e), SEM images of the nanodimple array formed on the aluminum substrate via anodizing at 25 and 40 V.

Results

The changes in current density with anodizing time at several voltages in a 0.3 M selenic acid solution at 293 K are shown in Fig. 1a. According to the growth model of anodic porous alumina, the current-time transient obtained via constant-voltage anodizing results in two overlapping oxide growths: barrier and porous layer formations[28]. The current density at the beginning of anodizing corresponded to a period of barrier layer (approximately 0.5 min, Fig. 1b), and the period after the barrier layer formation corresponded to porous layer formation. At 45 V, the current density increased rapidly to over 100 A m^{-2} within 1.5 min, and intense oxygen gas evolution was observed from the aluminum specimen because of "burning" by the electric current[29]. At other voltages, the current maintained a constant value after the initial stage because of steady growth of the anodic porous alumina. The plateau current densities at 25–40 V increased with anodizing voltage. During anodizing, reddish selenium was deposited on the counter electrode because of the reduction of selenate ions with hydrogen gas evolution (Supplementary Fig. S2). An SEM image of the vertical cross-section of the specimen obtained via typical anodizing is shown in Fig. 1c (here, the anodic oxide was etched in K$_3$[Fe(CN)$_6$]/NaOH solution for 20 s to clearly observe the porous layer). An approximately

5-µm-thick uniform anodic oxide film was formed on the aluminum substrate, and many nanopores grew linearly into the oxide. The obtained oxide consisted of amorphous Al$_2$O$_3$ containing 1.6 at% selenate ion (Supplementary Fig. S3). Figures unambiguously illustrate selenic acid's potential as a new electrolyte for anodic porous alumina fabrication.

When porous alumina is formed on aluminum via anodizing, its nanopores are generally created in a disorderly fashion in the anodic oxide. The nanopores then gradually become ordered at the oxide and aluminum substrate interface under appropriate applied voltages[15]. Therefore, studying the oxide and aluminum substrate interface is important for understanding the porous alumina's self-ordering behavior (Fig. 1d). Figure 1e displays SEM images of the interface after anodizing at 25 and 40 V for 60 min; the interface was exposed by selective oxide film removal. At 25 V, disordered dimples were distributed on the aluminum substrate. There dimples measured approximately 60 nm in mean diameter; however, the dimple's boundaries were little unclear because of insufficient oxide growth at the low electric current density. The mean nanodimple diameters increased linearly with anodizing voltage (Supplementary Fig. S4). Nevertheless, the dimple array was also disordered at 40 V despite the large current density. Self-ordering of anodic porous alumina can

generally be achieved at the maximum voltage required to induce high current density without burning[15,29]. To achieve self-ordering in selenic acid, we found that stirring vigorously at low temperature (273 K) during the anodizing was required to avoid oxide burning.

Current-time transients during selenic acid anodizing at 273 K is shown in Fig. 2a. The solution was stirred vigorously to suppress oxide breakdown. With appropriate solution cooling, steady anodic alumina growth without burning was observed at voltages as large as 48 V. Accordingly, the regularity of nanodimple arrays increased with the anodizing voltage (Fig. 2b), and it is clear that an ideal hexagonal nanodimple array was obtained at 48 V in 1 h. The corresponding convex nanostructures of the barrier layer was also obtained by aluminum substrate dissolution (Supplementary Fig. S5). Through SEM, the interpore distance was determined to be 112 nm at 48 V, and the obtained proportional constant (k = 2.33 nm V^{-1}) was consistent with those of other previously reported anodizing electrolytes[4].

Recently, Houser et al. postulated that metal-oxide interface motion occurs through the combination of ionic migration in the oxide and the stress-driven interface diffusion of metal atoms during anodizing[30,31]. Ono et al. reported that self-ordering anodizing is performed at a high electric field by choosing an adequate electrolyte[15]. Those researchers asserted that highly-ordered porous alumina can be formed at high voltages. Our results further demonstrated that the anodic oxide could be formed at up to 51 V in selenic acid with low electrolyte concentrations (0.1–0.03 M H$_2$SeO$_4$, Supplementary Fig. S6). However, the regularity of these anodic oxides is lower than that of the anodic oxides obtained at 48 V in 0.3 M selenic acid. Notably, the most appropriate voltage for cell ordering was 48 V during selenic acid anodizing, and this self-ordering was achieved via for 1 h. The self-ordering voltage and the corresponding interpore distance are summarized in Supplementary Fig. S7.

Figure 2c shows three-dimensional atomic force microscopy (AFM) images of the self-ordered nanodimple arrays formed on the aluminum substrate. The cell possessed six convex parts with approximately 20 nm in diameter at the apices of the hexagonal cell, and the bottom of each cell was hemispherical in shape. Using this nanodimple array as a template, a highly-ordered porous alumina from the surface to bottom can be obtained by selenic acid "re-anodizing" (two-step anodizing[1]). This re-anodizing can occur because the pores are generated at the nanodimple bottom in the initial anodizing stage. We found that the anodic porous alumina formed by two-step anodizing in selenic acid had the smallest 10-nm-scale pore diameter.

Figure 3a shows a typical surface image of the anodic porous alumina fabricated by two-step anodizing at 48 V for 10 min (first anodizing = 1 h, second anodizing = 10 min). The pore diameters are notably smaller than those of porous alumina obtained in the other previously reported electrolytes[27], and the diameters were 7.1–13.4 nm in the figure. The mean diameter of a 25-nanopore sample was measured to be 9.4 nm by SEM surface observations. This anodic porous alumina produced by two-step anodizing is the first report of a self-ordered anodic porous alumina with 10-nm-scale pores[26]. Vertical cross-sectional views of the porous alumina are shown in Fig. 3b, and the pores and the barrier layer are observable. The pore diameters were 9.3–12.0 nm, and the mean diameter was 10.3 nm. This value, obtained from the cross-sectional image, agrees well with the value measured at the surface (9.4 nm, Fig. 3a). We believe that the anodic oxide formed in the initial stage is not dissolved into the selenic acid solution during the 10-min short anodizing[32]. Similar porous alumina with 10-nm-scale pores were also obtained by anodizing for 1 h (Fig. 3c). The barrier layer thickness, measured from Fig. 3b, was approximately 54 nm, affording a calculated proportionality constant (1.13 nm V^{-1}) consistent with the previous reported
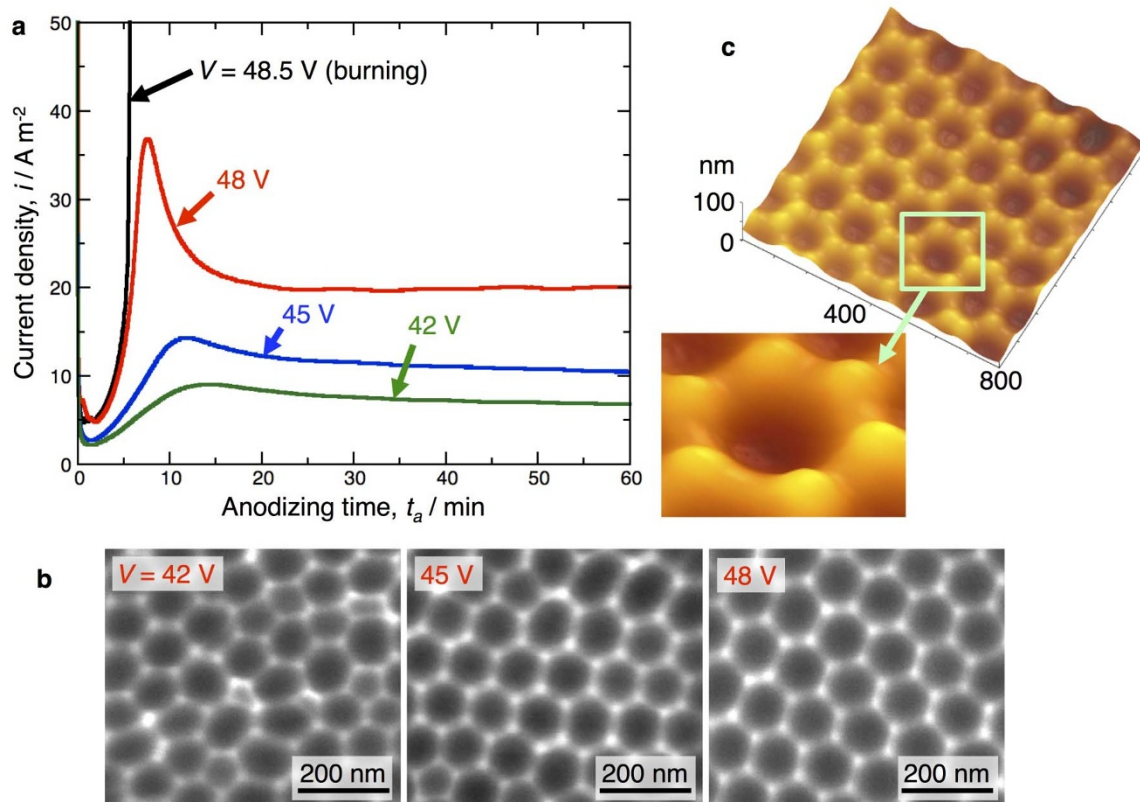

Figure 2 | **Self-ordering of anodic porous alumina formed in selenic acid solution at 273 K.** (a), Current-time transients during anodizing at 273 K and different constant voltages of 42–48.5 V. (b), SEM images of the nanodimple array formed on the aluminum substrate by anodizing at 42, 45, and 48 V. (c), Three-dimensional AFM height images of the self-ordered nanodimple array at low and high magnifications.
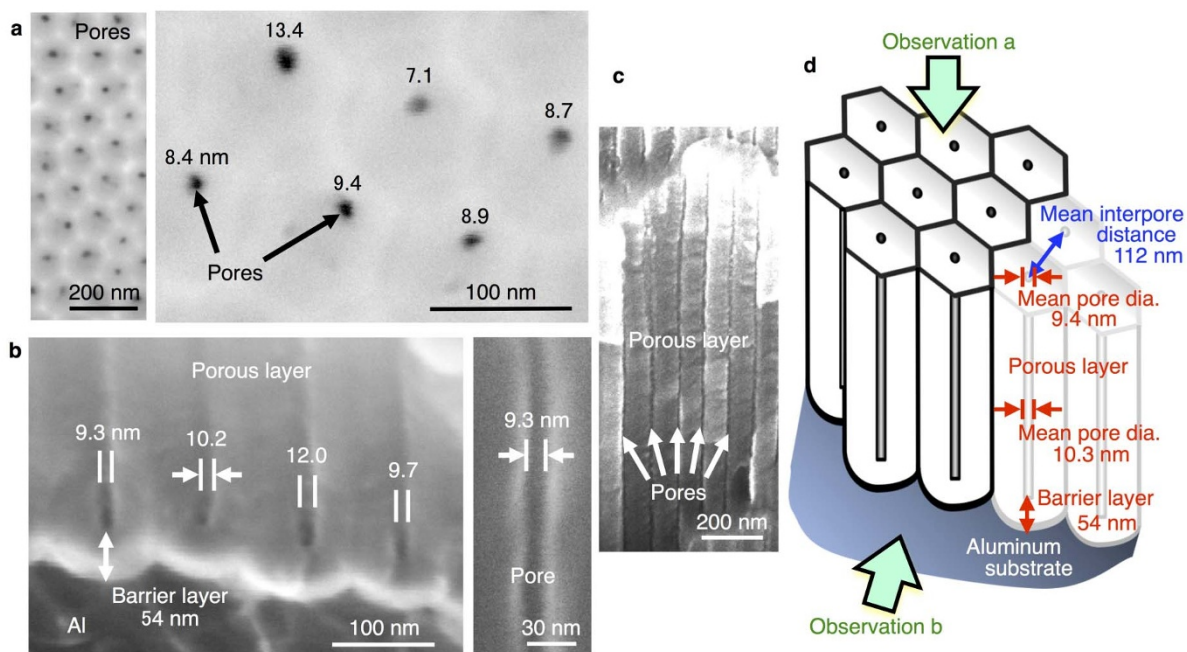
Figure 3 | Anodic porous alumina with 10-nm-scale pore arrays fabricated by two-step selenic acid anodizing. (a), Low- and high-magnification SEM images of the surface of the specimen that was anodized at 48 V for 10 min. The numbers in the figure represent the diameters of each nanopore. The mean pore diameter, averaged from 25 pores, is 9.4 nm. (b), SEM images of the vertical cross-section of the anodized specimen. Porous and barrier layers in the anodic oxide are visible. (c), SEM image of the vertical cross-section of the anodized specimen for 1 h. For panels (a) through (c), no conducting layer was deposited on the surface or cross-section of the anodized specimens to clearly observe the pores. (d), Nanostructural features of the self-ordered anodic porous alumina fabricated by two-step anodizing at 48 V.

value (1.15 nm V^{-1})[33]. The nanostructural features of the anodic porous alumina were summarized in Fig. 3d.

We combined the selenic acid anodizing technique with metal sputter deposition, and we found that the combination afforded interesting sub-10-nm-scale spacing. Figure 4a shows SEM images of the platinum layer deposited by sputtering onto the self-ordered anodic porous alumina that was fabricated by two-step selenic acid anodizing. Platinum metals were preferentially deposited on the six apices of each hexagonal cell (Supplementary Fig. S8), and equilateral triangle nanoparticles having a uniform shape were formed on each apex. From the high-magnification SEM image, we determined that each nanoparticle was separated by approximately 6.1 nm (Fig. 4b). Deposited platinum particles were easily removed by applying a small mechanical stress (Fig. 4a inset), and spaces were clearly visible between each nanoparticle. Sub-10-nm-scale gaps, such as those described in this technique, can be used in novel nanostructure applications such as transmitting optical signals in plasmonic devices.

Discussion

For an ideal self-ordering porous alumina, the density of pores, δ[pores cm^{-2}], can be calculated by the following equation[4]:

$$\delta = 1.155 \times 10^{14} / D_{int}^2 \qquad (1)$$

By substituting 112 nm for D_{int}, δ is estimated to be 9.2×10^9 pores cm^{-2}. The porosity of anodic alumina, α [%], can also be calculated using the following equation[34]:

$$\alpha = 3.628(r/D_{int})^2 \times 100 \qquad (2)$$

where r is the radius of nanopores. By substituting 5.2 nm for r, α is estimated to be 0.8%. Because our anodic oxide had the smallest pore diameter, the porosity was smaller than those of anodic alumina formed using typical anodizing electrolytes (3–10%)[4,34]. The pore
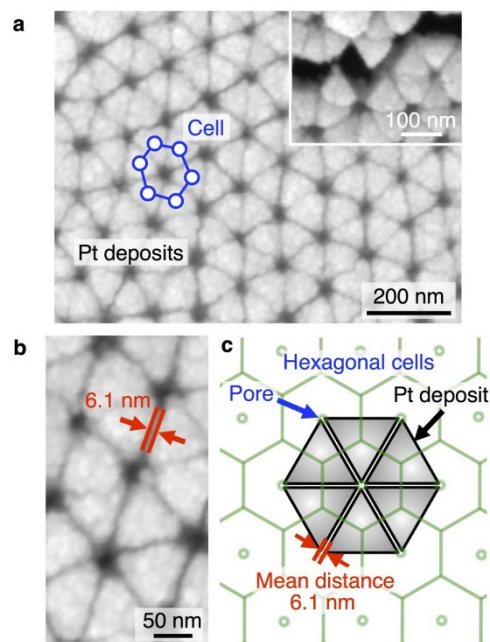

Figure 4 | Sub-10-nm-scale spacing and equilateral triangle nanoparticle fabrication. (a), SEM image of the highly ordered platinum nanostructure deposited on the anodic porous alumina by sputter deposition. The porous alumina was fabricated by the two-step selenic acid anodizing procedure shwon in Fig. 3a. The blue hexagonal schematic model represents a unit cell of the anodic porous alumina. (b), High-magnification SEM image of the platinum nanostructure on the anodic oxide. (c), Schematic model of the highly ordered platinum nanostructure on the anodic porous alumina.

diameter strongly depends on the anodic alumina dissolution rate at the pore bottom during anodizing[35]. To fabricate the smallest pores (less than 20 nm in diameter), sulfuric acid was generally selected as the anodizing electrolyte to date.

Masuda and co-workers investigated on the anodizing behavior of aluminum in highly concentrated H_2SO_4 solution at high temperature[36], and long-range-ordered anodic porous alumina with pore diameters of 12–18 nm and pore intervals of 25–30 nm was fabricated. Martin et al. worked on aluminum anodizing in H_2SO_4/ethylene glycol mixed solution, and obtained an ordered anodic porous alumina <15 nm in diameter and with a large aspect ratio[27]. These porous alumina films with 10-nm-scale pores have relatively small pore intervals (25–30 nm). Conversely, our porous alumina with 10-nm-scale pores possessed more larger pore interval (approximately 90–100 nm). Sulfuric acid possesses a similar chemical structure as selenic acid. When acids have different elements at the center from the same periodic table group, acid strengths generally decrease as the size of the central atom increases in the same oxidation state. Therefore, selenic acid is slightly less soluble than sulfuric acid. It is noted that the solubility has important effects on the pore diameter and interval during aluminum anodizing. Moreover, the solubility of selenic acid is very low at the experimental anodizing temperature of 273 K. Our results suggest that this weak solubility caused the formation of 10-nm-scale pores in the anodic porous alumina. However, further studies are required to understand the mechanism of pore formation via selenic acid anodizing under various electrochemical conditions. The large pore interval via selenic acid anodizing is not suitable for ultra-high density nanostructure fabrication such as magnetic recording media application. However, controlling and changing of the pore intervals in anodic porous alumina is important for photonics applications. The pore interval formed via selenic acid anodizing may be controlled under appropriate anodizing conditions (H_2SeO_4 concentration, temperature, voltage, etc.). The nanostructural features via selenic acid anodizing under these electrochemical conditions should be further investigated, and the results will be reported in the near future.

In summary, we synthesized the first anodic porous alumina formed using selenic acid as the electrolyte. Clearly, this electrolyte was identified after more than 40 years of using electrolytes in porous alumina fabrication. The self-ordered porous alumina could be rapidly produced (in 1 h) by selenic acid anodizing at 48 V. Our porous alumina possessed the smallest pore diameters reported to date (10-nm-scale pores). The use of selenic acid in the anodizing at low temperature without any special electrochemical equipment and pretreatment was critical for achieving this small pore diameter. The solubility in selenic acid solution at low temperature has important effects on the pore diameter and interval during aluminum anodizing. The combination of selenic acid anodizing and metal sputter deposition allowed the formation of sub-10-nm-scale gaps. We strongly believe that this new anodizing electrolyte will be used for fabricating various nanoapplications with interesting 10-/sub-10-nm-scale features such as nanorods, nanotubes, nanocrystals, and nanodevices.

Methods

Pretreatment of the aluminum specimens. Highly pure aluminum foil (Showa Aluminum Co., Japan, 99.99 mass%, 110 μm thick, impurities: Fe 10 ppm, Si 9 ppm, and Cu 57 ppm) was used as the anodizing specimen. The foils was cut into 20 mm × 20 mm pieces with a handle and then ultrasonically degreased in ethanol for 10 min. The degreased specimens were electrochemically polished in a 13.6 M CH_3COOH/ 2.56 M $HClO_4$ solution (280 K) at a constant voltage of 28 V for 60 s. An aluminum plate was used as the counter electrode during electropolishing. After polishing, the specimens were washed with distilled water and then dried in a desiccator.

Selenic acid anodizing. The electropolished specimens were immersed in 0.03– 0.3 M selenic acid solutions (273–293 K, 100–130 mL, pH of 0.3 M selenic acid solution is 0.63 at 293 K) and set in the parallel positions with 15 mm from a glassy carbon counter electrode (Tokai Carbon Co., Japan, 1 mm thick). After setting, the specimens were anodized up to 180 min at a constant voltage of 25–51 V. During the

anodizing, the selenic acid solutions were vigorously stirred with a magnetic stirrer, and the current densities were measured using a digital multi-meter (DMM4040, Tektronix). After anodizing, the specimens were washed with distilled water and then dried in a desiccator. The anodized specimen was immersed in a 1.0 M $SnCl_4$ solution at room temperature to completely dissolve the aluminum substrate, and a convex oxide nanostructure was obtained by lift-off. For two-step anodizing, the anodized specimens were immersed in a 0.20 M CrO_3/0.54 M H_3PO_4 solution (353 K) for 20 min to selectively dissolve the anodic oxide, and a nanodimple array was formed on the aluminum substrate via dissolution. Afterward, the aluminum specimens were anodized again in a 0.3 M selenic acid solution for 60 min.

Characterization of the anodic porous alumina. The structural changes induced in the specimens by anodizing were examined by field-emission scanning electron microscopy (JSM-6500F and JIB-4600F/HKD, JEOL), field emission electron probe microanalysis (JXA-8530F, JEOL), and AFM (Nanocute, Hitachi). For vertical cross sections, two treated specimens were prepared. a) For microscale observations, the specimens were embedded in an epoxy resin, polished mechanically, and then immersed in a 0.25 M $K_3[Fe(CN)_6]$/4.17 M NaOH solution at room temperature for 20 s to clearly observe the nanoporous layer in the anodic oxide. b) For nanoscale observation, the specimens were mechanically cut in liquid nitrogen. No electroconductive metal deposition was performed for the surface and cross-sectional observations of the anodic porous alumina, except for Supplementary Fig. S5. The phase compositions of the anodized specimen and deposits on the counter electrode were determined using X-ray diffraction (XRD, XpertPro, Phillips) analysis.

Fabrication of palatium porous nanoparticles with sub-10-nm-scale spaces. The self-ordered anodic porous alumina formed by two-step anodizing was set in a parallel position 25 mm from a platinum sputtering target (99.99 at%) on a sputter coater (MSP-1S, Vacuum Device Co., Japan), and then platinum was sputter coated on the anodic porous alumina at 40 mA for 10 min (coating rate on flat surface: 25 nm min^{-1}).

1. Masuda, H. & Fukuda, K. Ordered metal nanohole arrays made by a two-step replication of honeycomb structures of anodic alumina. *Science* **268**, 1466–1468 (1995).
2. Masuda, H. & Satoh, M. Fabrication of gold nanodot array using anodic porous alumina as an evaporation mask. *Jpn. J. Appl. Phys.* **35**, L126–L129 (1996).
3. Yamaguchi, A. N. *et al.* Self-assembly of a silica-surfactant nanocomposite in a porous alumina membrane. *Nature Materials* **3**, 337–341 (2004).
4. Lee, W., Ji, R., Gösele, U. & Nielsch, K. Fast fabrication of long-range ordered porous alumina membranes by hard anodization. *Nature Materials* **5**, 741–747 (2006).
5. Jha, H., Kikuchi, T., Sakairi, M. & Takahashi, H. Synthesis of aluminum oxy-hydroxide nanofibers from porous anodic alumina. *Nanotechnology.* **19**, 395603 (6pp) (2008).
6. Yamauchi, Y., Nagaura, T. & Inoue, S. Oriented growth of small mesochannels utilizing a porous alumina substrate: preparation of continuous film with standing mesochannels. *Chem. Asian J.* **4**, 1059–1063 (2009).
7. Yamauchi, Y. *et al.* Generation of electron moiré fringes on designed nanoporous anodic alumina films and their replicated Ni cone arrays: exploration of domain sizes and nanopore arrangements. *J. Phys. Chem. C* **113**, 9632–9637 (2009).
8. Yamauchi, Y., Nagaura, T., Ishikawa, A., Chikyow, T. & Inoue, S. Evolution of standing mesochannels on porous anodic alumina substrates with desiged conical holes. *J. Am. Chem. Soc.* **130**, 10165–10170 (2008).
9. Zhao, X. *et al.* Nanocontainers made of various materials with tunable shape and size. *Sci. Rep.* **3**, 2238 (2013).
10. Kikuchi, T., Wachi, Y., Sakairi, M. & Suzuki, R. O. Aluminum bulk micromachining through an anodic oxide mask by electrochemical etching in an acetic acid/perchloric acid solution. *Microelectron. Eng.* **111**, 14–20 (2013).
11. Lin, Q., Hua, B., Leung, S., Duan, X. & Fan, Z. Efficient light absorption with integrated nanopillar/nanowell arrays for three-dimensional thin-film photovoltaic applications. *ACS Nano* **3**, 2725–2732 (2013).
12. Thompson, G. E., Furneaux, R. C., Wood, G. C., Richardson, J. A. & Gode, J. S. Nucleation and growth of porous anodic films on aluminium. *Nature* **272**, 433–435 (1978).
13. Thompson, G. E. & Wood. Porous anodic film formation on aluminum. *Nature* **290**, 230–232 (1981).
14. Furneaux, R. C., Rigby, W. C. & Davidson, A. P. The formation of controlled-porosity membranes from anodically oxidized aluminum. *Nature* **337**, 147–149 (1989).
15. Ono, S., Saito, M. & Asoh, H. Self-ordering of anodic porous alumina formed in organic acid electrolytes. *Electrochim. Acta* **51**, 827–833 (2005).
16. Chu, S. Z. A. *et al.* Large-scale fabrication of ordered nanoporous alumina films with arbitrary pore intervals by critical-potential anodization. *J. Electrochem. Soc.* **153**, B384–B391 (2006).
17. Kikuchi, T., Wachi, Y., Takahashi, T., Sakairi, M. & Suzuki, R. O. Fabrication of a meniscus microlens array made of anodic alumina by laser irradiation and electrochemical techniques. *Electrochim. Acta* **94**, 269–276 (2013).
18. Li, A. P., Müller, F., Birner, A., Nielsch, K. & Gösele, U. Polycrystalline nanopore arrays with hexagonal ordering on aluminum. *J. Vac. Sci. Technol. A.* **17**, 1428–1431 (1999).

19. Lee, W., Nielsch, A. & Gösele, U. Self-ordering behavior of nanoporous anodic aluminum oxide (AAO) in malonic acid anodization. *Nanotechnology.* **18**, 475713 (8 pp) (2007).

20. Fukushima, T., Fukuda, Y., Ito, G. & Sato, Y. Anodic oxidation and local corrosion of aluminum in mono-carboxylic acids. *J. Surf. Fin. Soc. Jpn.* **25**, 319–326 (1970).

21. Fukushima, T., Fukuda, Y., Ito, G. & Okada, M. Anodic oxidation of aluminum in aqueous solution of dicarboxylic acids. *J. Surf. Fin. Soc. Jpn.* **25**, 447–452 (1974).

22. Fukushima, T., Fukuda, Y., Ito, G. & Miyoshi, M. Anodic oxidation of aluminum at high current density in the aqueous solution of hydroxycarboxylic acids. *J. Surf. Fin. Soc. Jpn.* **25**, 537–541 (1974).

23. Masuda, H., Hasegawa, F. & Ono, S. Self-ordering of cell arrangement of anodic porous alumina formed in sulfuric acid solution. *J. Electrochem. Soc.* **144**, L127–L130 (1997).

24. Masuda, H., Yada, K. & Osaka, A. Self-ordering of cell configuration of anodic porous alumina with large-size pores in phosphoric acid solution. *Jpn. J. Appl. Phys.* **37**, L1340–L1342 (1998).

25. Jessensky, O., Müller, F. & Gösele, U. Self-organized formation of hexagonal pore arrays in anodic alumina. *Appl. Phys. Lett.* **72**, 1173–1175 (1998).

26. Sulka, G. D. & Hnida, K. Distributed bragg reflector based on porous anodic alumina fabricated by pulse anodization. *Nanotechnology* **23**, 075303 (8 pp) (2012).

27. Martin, J., Manzano, C. V., Caballero-Calero, O. & Martin-Gonzalez, M. High-aspect-ratio and highly ordered 15-nm porous alumina templates. *ACS Appl. Mater. Inter.* **5**, 72–79 (2013).

28. Hoar, T. P. & Yahalom, J. The initiation of pores in anodic oxide films formed on aluminum in acid solutions. *J. Electrochem. Soc.* **110**, 614–621 (1963).

29. Ono, S., Saito, M., Ishiguro, M. & Asoh, H. Controlling factor of self-ordering of anodic porous alumina. *J. Electrochem. Soc.* **151**, B473–B478 (2004).

30. Houser, J. E. & Hebert, K. R. The role of viscous flow of oxide in the growth of self-ordered porous anodic alumina films. *Nature Materials* **8**, 415–420 (2009).

31. Hebert, K. R., Albu, S. P., Paramasivam, I. & Schmuki, P. Morphological instability leading to formation of porous anodic oxide films. *Nature Materials* **11**, 162–166 (2012).

32. Zhang, J., Kielbasa, J. K. & Carroll, D. L. Controllable fabrication of porous alumina templates for nanostructures synthesis. *Mater. Chem. Phys.* **122**, 295–300 (2010).

33. Garcia-Vergara, S. J. P. *et al.* Mechanical instability and pore generation in anodic alumina. *Proc. R. Soc. A* **462**, 2345–2358 (2006).

34. Nielsch, K., Choi, J., Schwirn, K., Wehrspohn, R. B. & Gösele, U. Self-ordering regimes of porous alumina: The 10% porosity rule. *Nano Letters* **2**, 677–680 (2002).

35. Lee, W. U. *et al.* Structural engineering of nanoporous anodic aluminum oxide by pulse anodization of aluminum. *Nature Nanotechnology* **3**, 234–239 (2008).

36. Masuda, H., Takenaka, K., Ishii, T. & Nishio, K. Long-range-ordered anodic porous alumina with less-than-30 nm hole intervals. *Jpn. J. Appl. Phys.* **45**, L1165–L1167 (2006).

Author contributions

O.N. and T.K. designed and performed the selenic acid anodizing, analyzed data, and wrote the manuscript. S.N. and R.O.S. contributed to the analysis and the manuscript writing.

Additional information

Supplementary information accompanies this paper at http://www.nature.com/scientificreports

Competing financial interests: The authors declare no competing financial interests.

How to cite this article: Nishinaga, O., Kikuchi, T., Natsui, S. & Suzuki, R.O. Rapid fabrication of self-ordered porous alumina with 10-/sub-10-nm-scale nanostructures by selenic acid anodizing. *Sci. Rep.* **3**, 2748; DOI:10.1038/srep02748 (2013).